Powder Technology 246 (2013) 16–25

Contents lists available at SciVerse ScienceDirect

Powder Technology

journal homepage: www.elsevier.com/locate/powtec

Numerical investigation of effect of electrostatic forces on the hydrodynamics of gas–solid fluidized beds

M.A. Hassani, R. Zarghami, H.R. Norouzi, N. Mostoufi *

Process Design and Simulation Research Center, School of Chemical Engineering, College of Engineering, University of Tehran, P.O. Box 11155-4563, Tehran, Iran

ARTICLE INFO

Article history:
Received 4 February 2013
Received in revised form 30 April 2013
Accepted 3 May 2013
Available online 10 May 2013

Keywords:
Fluidized bed
Discrete element method
Computational fluid dynamics
Electrostatic force
Mixing

ABSTRACT

A 3D discrete element method (DEM) coupled with computational fluid dynamics (CFD) model was developed for studying the effect of electrostatic forces between particles on fluidization hydrodynamics. To validate this code, bubble diameters in the single bubble injection and freely bubbling regimes were compared with experimental values and acceptable agreement was observed. The simulation results showed that by increasing the charge of mono-charged particles into the bed, the bubble size and solid diffusion coefficient decrease and distribution of porosity and particles circulation also change and bed tends toward more homogeneity. By adding bipolar charged particles into the bed, bubble size, solids diffusivity and voidage distribution approach to that of the neutral bed and particles tend to form chains of connected particles.

1. Introduction

Fluidized beds provide a good solids mixing that enhances the bed uniformity during its operation. However, electrification of particles may change the mixing quality of solids in the bed [1]. Particle charging is caused by frequent particle–particle, wall–particle collisions and gas–solid friction which are unavoidable in fluidized beds [2]. Electrostatic charges can affect hydrodynamics of the fluidized bed, e.g., bubble size, void fraction of bubble and emulsion phases and solid flow pattern. Moreover, if electrostatic charge on particles reaches a critical value, particles adhere to the reactor wall and wall sheeting occurs [3].

Electrification of particles in gas–solid systems has been studied by many researchers. Boland and Geldart studied effect of mean particle size and relative humidity on the rate of charge generation and dissipation in a gas–solid fluidized bed [4]. Baron et al. studied the effect of electrostatic charge on entrainment of silica sand particles at various relative humidity and showed that an increase in the relative humidity decreases electrostatic forces [5]. Matsusaka and Masuda offered a novel method for measurement of electric current and calculation of mass flow rate and charge-to-mass ratio of particles in gas–solid pipe flows by theoretical equations [6]. Matsusaka et al. concluded that bipolar charge distribution depends on the material of particles in the gas–solid pipe flow [7]. Experimental observations have also shown that the particles with the same material properties may gain negative or positive charges (bipolar) depending on their relative sizes in the system [8–10]. Cartwright et al. showed that fine particles tend to be charged negatively, while larger particles gain positive charge in a pneumatic conveying system [8]. Sowinski et al. developed Faraday cup method for evaluating the charge to mass ratio in a fluidized bed with a wide size distribution of polyethylene particles and observed bipolar charged particles [10].

There are many investigations about particle electrification in gas–solid systems [2,4,6–15]. However, fewer experimental studies were performed on the bed hydrodynamics and solid mixing [5,16–18]. A better understanding of bed hydrodynamics and solid flow pattern can be achieved through numerical simulation. Available mathematical model for investigating gas–solid systems can be grouped into two main categories: Eulerian–Eulerian [19] and Eulerian–Lagrangian approaches [20]. Eulerian–Lagrangian approach is the combined computational fluid dynamics (CFD) and discrete element method (DEM). In this modeling approach, particles are considered as individual entities and their motions are described by Newton's second law of motion while the gas phase is considered as a continuum and its motion is described by the local-averaged Navier–Stokes equations. This method has been recognized as an effective model to study the fundamentals of particle–fluid flow [20] and granular systems [21]. Hogue et al. used the DEM to simulate electrification of particles as a result of rolling on an inclined plane [22]. Lim et al. coupled the DEM with CFD to study the influence of electrostatic force on flow of solids in a pneumatic conveying system. They assumed a constant charge for each particle to evaluate the electrostatic force between particles [23]. Rokkam et al. coupled an electrostatic model with multi-fluid model to investigate the effect of electrostatic forces on hydrodynamics of fluidized bed and showed that segregation induced by electrostatic forces can affect the entrainment of fines [24]. Jalalinejad et al. compared single bubble rise in charged and uncharged fluidized bed by the two-fluid model [25].

* Corresponding author. Tel.: +98 21 6696 7797; fax: +98 21 6696 7781.
E-mail address: mostoufi@ut.ac.ir (N. Mostoufi).

0032-5910/$ – see front matter © 2013 Elsevier B.V. All rights reserved.
http://dx.doi.org/10.1016/j.powtec.2013.05.007

Effects of electrostatic forces on the fluidized bed hydrodynamics as well as solid flow pattern are less studied. Good solid mixing is an important parameter that ensures a uniform distribution of product quality, solid temperature or concentration in the bed. In addition, the hydrodynamic elements like bubble motion and bed porosity directly influence the solid flow pattern/mixing in the bed [26,27]. In this study, effect of electrostatic forces on bubble hydrodynamics, bed porosity, solids diffusivity and solid circulation length were studied. Two sets of simulations were performed: a bed filled with mono-charged particles and bipolar charged particles. A 3D CFD–DEM code was used to calculate inter-particle electrostatic forces among charged particles and between charged particles and wall [28].

2. Numerical model

In the CFD–DEM approach, the gas phase is considered as a continuous phase and solids are considered as discrete particles [29]. Full descriptions of governing equations and numerical implementation are described elsewhere [20,30–32] and a brief description is presented here.

2.1. Governing equations for particles

There are various methods for DEM simulation in literature [33]. In the present study, the soft sphere DEM was used [34]. Two types of motions, i.e., translational and rotational, are considered for each particle. The translational motion of each particle is described as follows:

$$m_i \frac{d\vec{v}_i}{dt} = m_i \frac{d^2\vec{r}_i}{dt^2} = \sum_{j=1}^{n_c} \vec{f}_{ij}^{\,c} + \vec{f}_{pf,i} + m_i\vec{g} + \sum_{k}^{n_k} \vec{f}_{e,ik} + \vec{f}_{e,i-wall} \quad (1)$$

The terms in the right-hand side of Eq. (1) are contact, fluid-drag, gravity, inter-particle electrostatic and particle–wall electrostatic forces, respectively, and are given in Table 1.

In a granular system, a particle may interact with more than one particle in each instance. Thus, pair-wise contact forces are summed over n_c particles which are in contact with particle i. Similarly, a charged particle may interact with surrounding particles (n_k particles) via electrostatic forces. In this case, particles which are not in contact with particle i should also be considered. In the present work, the Verlet list was utilized for detecting long-range contact interactions in which a cut-off radius is considered for inter-particle forces. All particles around the target particle that lie within a sphere with radius $R_{cut\text{-}off}$ are added to the Verlet list of the target particle (Fig. 1). The main advantage of this method is that particles in the Verlet list of each particle would stay in this list for a few time steps. Thus, it is not required to update the Verlet list in each time step. Yao et al. [35] combined the Verlet list algorithm and cell linked list by cell decomposition to speed up the construction of the Verlet list. This method was used in this work. Lower CPU time would be required for constructing the Verlet list and the speed of the algorithm was increases by a factor of 2 to 3. The radius $R_{cut\text{-}off}$ for the target particle was considered as the distance for which the electrostatic force becomes less than 5% of the weight of the particle.

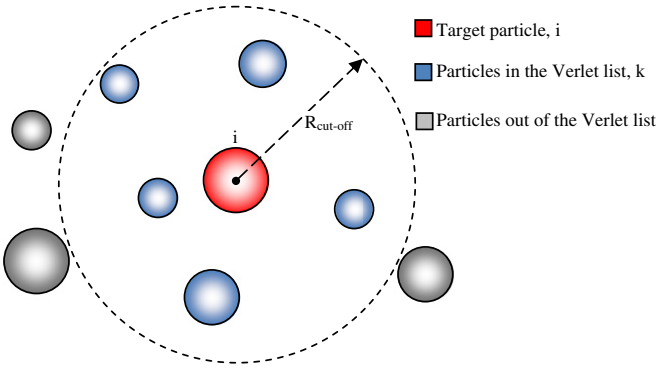

Fig. 1. The Verlet list of target particle i.

The attractive particle–wall electrostatic force arises from image charge effect. When a charged particle is close to a conductive wall, a charge would be induced on the other side of the wall with an opposite sign. This leads to an attractive force between the particle and the wall which causes wall sheeting of particles.

The rotational motion of each particle is governed by the following equation:

$$I_i \frac{d\vec{\omega}_i}{dt} = \sum_{j=1}^{n_c} \left(\vec{M}_{ij}^{\,t} + \vec{M}_{ij}^{\,r} \right) \quad (2)$$

Inter-particle forces cause a torque in tangential direction, $\vec{M}_{ij}^{\,t}$, is the origin of particle rotation. Parameter $\vec{M}_{ij}^{\,r}$ is another torque acting on particle i, known as the rolling resistant torque, which always opposes the rotation of the particle.

Table 1
Equations of forces acting on particle i.

Contact forces	Normal	$\vec{f}_{ij}^{\,n}$	$-(k_n\delta_n)\vec{n}_{ij} - \left(\eta_i \vec{v}_{r,ij}.\vec{n}_{ij}\right)\vec{n}_{ij}$
	Tangential	$\vec{f}_{ij}^{\,t}$	$-\left(\min\left(\mu\left\vert\vec{f}_{ij}^{\,n}\right\vert, \left\vert k_t\delta_t\vec{t}_{ij}\right\vert\right)\frac{\delta_t}{\vert\delta_t\vert}\right)\vec{t}_{ij} - \eta_i\vec{V}_{t,ij}$
Torque	Inter-particle	$\vec{M}_{ij}^{\,t}$	$\vec{R}_i \times \vec{f}_{ij}^{\,t}$
	Rolling	$\vec{M}_{ij}^{\,r}$	$-\mu_r R_{p,i}\left\vert f_{ij}^{n}\right\vert\hat{\omega}_{ij}$
Electrostatic forces	Particle–particle	$\vec{f}_{e,ik}$	$k_e \frac{q_i q_k\left(\vec{r}_i - \vec{r}_k\right)}{\left\vert\vec{r}_i - \vec{r}_k\right\vert^3}$
	Particle–wall	$\vec{f}_{e,i-wall}$	$-k_e \frac{q_i^2\left(\vec{r}_i - \vec{r}_{wall}\right)}{4\left\vert\left(\vec{r}_i - \vec{r}_{wall}\right)^3\right\vert}$
Fluid drag force [47]		$\vec{f}_{d,i}$	$\hat{f}_{d,i} = 3\pi d_{p,i}\mu_f\varepsilon\left(\vec{u} - \vec{v}_i\right)$
			$\hat{f}_{d,i} = \frac{C_d}{24}Re\varepsilon^{-\chi}$
			$\chi = 3.7 - 0.65\exp(-0.5(1.5 - \log_{10}Re))$
			$C_d = (0.63 + 4.8Re^{-1/2})^2$

where: $\vec{R}_i = \vec{r}_j - \vec{r}_i$, $\vec{n}_{ij} = \frac{R_i}{\left\vert\vec{R}_i\right\vert}$, $\vec{v}_{r,ij} = \vec{v}_i - \vec{v}_j$, $\hat{\omega}_{ij} = \frac{\vec{\omega}_i - \vec{\omega}_j}{\left\vert\vec{\omega}_i - \vec{\omega}_j\right\vert}$, $\mathrm{Re} = \frac{\rho_f d_{p,i}\varepsilon\left\vert\vec{u} - \vec{v}_i\right\vert}{\mu_f}$, $\vec{V}_{t,ij} = \left(\vec{v}_{r,ij}.\vec{t}_{ij}\right) + \left(\vec{\omega}_i \times \vec{R}_i - \vec{\omega}_j \times \vec{R}_i\right)$,.